Renewable Energy, Environment, and Power Quality Journal (REE&PQJ)
ISSN:3020-531X
Volume 26, July 2026

Real-Time Multi-Objective Optimization for Reactive Power Dispatch in Islanded Power System

Carolina M. Martín[1], Francisco Arredondo[1], Santiago Arnaltes[1], Jaime Alonso-Martínez[1] and José Luis Rodríguez-Amenedo[1]

[1] Departamento de Ingeniería Eléctrica
Universidad Carlos III de Madrid
Campus de Leganés - Leganés, 28911 Madrid (Spain)

Abstract.

This paper proposes a real-time (RT) optimization strategy for managing reactive power reserves in islanded power systems, explicitly maintaining safe margins from voltage limits. Existing formulations, dominated by objective functions aimed at minimizing losses, are shown to systematically drive bus voltages close to their upper admissible limits, potentially reducing operational margins and increasing the risk of overvoltage tripping. This work conducts a comparative study using three alternative multi-objective functions aimed at reducing power losses and mitigating voltage saturation: one previously proposed in the literature and two new formulations presented in this paper to overcome the limitations identified in the first. The analysis is conducted within a realistic real-time hardware-in-the-loop (HIL) optimization laboratory environment (RTOLab) and assessed over a full-day operation with a 5-minute execution interval. The optimization problem computes reactive power and voltage setpoints for power plant controllers in real time and performs redispatch actions as necessary to ensure secure operation. Results demonstrate that the two multi-objective functions proposed in this paper, aimed at avoiding voltage limits or penalizing reactive power reserve utilization, have a limited impact on system losses and exhibit operational robustness in RT optimization–based applications.

Keywords. Optimal reactive power management, voltage control, optimal control setpoints, real-time optimization, hardware-in-the-loop simulation.

Nomenclature

A. Sets

$\mathcal{N}$ Set of buses in the system
$\mathcal{G} \subset \mathcal{N}$ Subset of buses with generators
$\mathcal{D} \subset \mathcal{G}$ Subset of buses with dispatchable power plants
$\mathcal{R} \subset \mathcal{G}$ Subset of buses with renewable generation units

B. Parameters

$C_i^{D,up}$ Cost coefficient associated with the upward active power redispatch of generator at bus i, $\forall i \in \mathcal{D}$ [m.u./MWh]
I_{ik}^{max} Upper current limit of the line connecting buses i and k, $\forall i,k \in \mathcal{N}$ [p.u.]
$P_i^{D,min}, P_i^{D,max}$ Minimum and maximum active power limits of generator at bus i, $\forall i \in \mathcal{D}$ [p.u.]
$P_i^{D,sch}$ Scheduled active power of generator at bus i, $\forall i \in \mathcal{D}$ (provided by EMS/market) [p.u.]
P_i^L, Q_i^L Forecasted active and reactive power load at bus i, $\forall i \in \mathcal{N}$ [p.u.]
P_i^R Forecasted available renewable power at bus i, $\forall i \in \mathcal{R}$ [p.u.]
$Q_i^{G,min}, Q_i^{G,max}$ Minimum and maximum reactive power limits of generator at bus i, $\forall i \in \mathcal{G}$ [p.u.]
$Q_i^{G,ref}$ Reference reactive power of generator i, $\forall i \in \mathcal{G}$ [p.u.]
T_{opt} Optimization interval [min]
V_i^{min}, V_i^{max} Minimum and maximum allowable bus voltage magnitude at bus i, $\forall i \in \mathcal{N}$ [p.u.]
V_i^{ref} Reference voltage at bus i, $\forall i \in \mathcal{N}$ [p.u.]
α, β, γ Weighting factors for objective function terms
Y_{ik}, φ_{ik} Magnitude and angle of element (i,k) of the admittance matrix, $\forall i,k \in \mathcal{N}$ [p.u., rad]

C. Variables

i_{ik} Current in line connecting nodes i and k, $\forall i,k \in \mathcal{N}$ [p.u.]
f_i^c Curtailment factor for renewable generator at bus i, $\forall i \in \mathcal{R}$ [p.u.]
$p_i^{D,sp}$ Active power setpoint after redispatch of generator at node i, $\forall i \in \mathcal{D}$ [p.u.]
p^{loss} Active power losses in the system [p.u.]
q_i Reactive power setpoint at node i, $\forall i \in \mathcal{N}$ [p.u.]
v_i, θ_i Voltage magnitude and angle at bus i, $\forall i \in \mathcal{N}$ [p.u., rad]
$\Delta p_i^{D,up}, \Delta p_i^{D,down}$ Upward and downward active power redispatch of generator at node i, $\forall i \in \mathcal{D}$ [p.u.]
Δv_{max} Auxiliary variable to determine the maximum voltage deviation [p.u.]

1. Introduction

The increasing penetration of converter-interfaced generation is introducing new challenges in power system operation. In response, online optimization techniques that enable real-time (RT) operational adjustments and explicitly account for the variability of renewable energy sources (RES) have gained increasing attention [1]. Among these techniques, approaches based on optimal power flow (OPF), commonly referred to as RT-OPF, have emerged as a key tool for RT operational control [2], [3]. Additionally, current system operation typically relies on an economic scheduling stage that is usually determined by a market mechanism or an energy management system (EMS), which fixes active power setpoints in advance. RT operation then acts as a corrective layer, computing optimal controllable setpoints to ensure secure system operation while accounting for current system conditions and constraints [4], [5].

In this context, cost and active power losses minimization are commonly adopted objectives in both scheduling and RT optimization formulations [6], [7]. While such objectives promote efficient operation, they may also lead to specific operating patterns. In particular, losses minimization tends to exploit the voltage dependence of system losses, systematically driving bus voltages towards their upper admissible limits. Although these operating points satisfy static operational constraints, persistent operation close to voltage limits may reduce operational margins and increase sensitivity to disturbances. Recent operational events have highlighted the importance of adequate voltage management. For instance, the April 2025 Iberian Peninsula blackout has been associated with overvoltage-related operational challenges [8].

Accordingly, several works have addressed reactive power and voltage profile management [9], [10] and their relationship with system losses [11] by introducing additional voltage constraints, stability indices, or explicit voltage and reactive power security margins within OPF-based formulations [12], [13].

This paper investigates this phenomenon within a realistic RT optimization framework, which determines reactive power and voltage setpoints based on the market/EMS economic dispatch, by analyzing the impact of the objective function. A loss-cost-minimizing formulation is initially examined to illustrate its tendency to produce voltage-saturated operating points. Subsequently, three alternative multi-objective formulations are compared to mitigate this behaviour. The first introduces a quadratic penalization of voltage deviations, a strategy widely adopted in the literature and commonly referred to as voltage flattening. However, results show that some voltage dispersion remains, as this formulation penalizes average deviations rather than explicitly limiting extreme values, and additionally, reduces the system's reactive power margin.

To overcome these drawbacks, this paper extends our previous work [5]—which focused on the minimization of losses and redispatch costs and validation of the RT optimization framework—by proposing two additional formulations: one that minimizes the maximum voltage deviation across the system, and a combined objective that penalizes both voltage deviations and reactive power usage.

The proposed approach is applied to the Lanzarote-Fuerteventura isolated power system, in the Canary Islands, Spain. All formulations are implemented and evaluated in RTOLab, a RT optimization laboratory environment that enforces realistic execution and data-handling constraints. The comparison is carried out over a full 24-hour period with a 5-minute execution interval. Performance is assessed in terms of voltage profiles, system losses, reactive power utilization, and a steady-state robustness indicator based on the minimum eigenvalue of the power-flow Jacobian.

2. Real-Time Operational Framework and Validation Environment

A. Real-Time Operational Workflow

Fig. 1 details the workflow of the implemented control strategy, which is designed to operate as a RT complementary layer beneath an existing market- or EMS-based scheduling process. At each execution interval, the optimization problem receives as inputs the scheduled active power setpoints of dispatchable units, short-term forecasts of load demand and renewable generation, and updated asset limits and grid conditions. The optimization problem computes corrective active power redispatch actions together with reactive power and/or voltage magnitude setpoints for power plants, ensuring that operational constraints are satisfied while optimizing the selected objective function. The optimization is executed according to the defined optimization interval, T_{opt}, which must be selected to ensure a time resolution consistent with RT operational requirements, allowing the proposed strategy to be realistically integrated. The optimization problem is implemented using Pyomo and solved with IPOPT. At each execution, the problem is instantiated with the latest forecasts and scheduled setpoints, solved, and the resulting control actions are transmitted to the lower layers via Modbus.

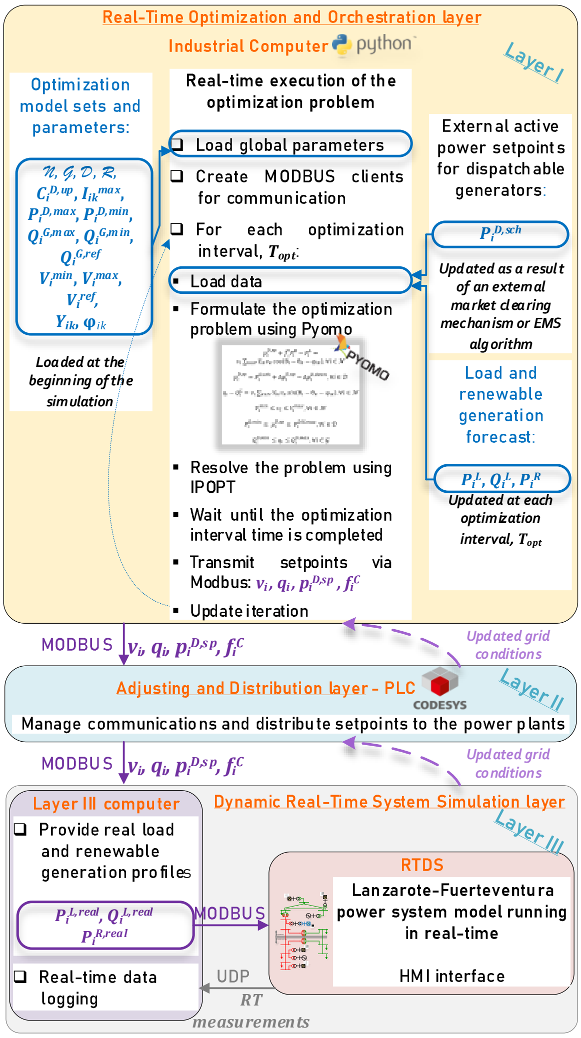

Fig. 1. RT optimization-based control architecture in RTOLab

B. RTOLab Architecture

The RT validation experiments of the proposed strategy are conducted in RTOLab, a RT HIL laboratory environment specifically designed to validate optimization and control algorithms under realistic system conditions. RTOLab has a modular three-layer architecture: a Real-Time Optimization and Orchestration layer (Layer I), an Adjusting and Distribution layer (Layer II), and a Dynamic Real-Time System Simulation layer (Layer III). Fig. 2 shows the hardware setup, including an industrial computer (IC) for the first layer, a programmable logic controller (PLC) for the second, and a real-time digital simulator (RTDS) with a dedicated computer for the third.

Layer I is responsible for data acquisition and hosts the RT optimization algorithm, which is implemented in Python and executed periodically according to the selected time horizon. Layer II distributes the computed setpoints to the system's assets and manages communication between the upper and lower layers. Finally, Layer III emulates the power system response by executing detailed electromagnetic transient (EMT) dynamic models of the assets and the grid in real time on the RTDS. Simultaneously, the dedicated computer continuously updates the system operating conditions to reproduce realistic RT system behavior on the RTDS. Data exchange among layers is handled through standardized communication protocols, allowing the optimization algorithm to receive updated system states and to transmit the computed setpoints within each execution cycle.

3. Real-Time Optimization Formulation

A. Base Case: Losses and Redispatch Cost Minimization

In the base case, the objective function aims at minimizing system losses together with the cost associated with corrective upward active power redispatch. This formulation reflects a RT operational objective in which deviations from scheduled operation are penalized while technical efficiency is promoted. The objective function *(Obj I)* can be expressed as:

$$min\, f\left(\Delta p_i^{D,up}, p^{LOSS}\right) = \sum_{i\in\mathcal{D}} C_i^{D,up} \Delta p_i^{D,up} + p^{loss} \quad (1)$$

where p^{loss} denotes total active power losses and is calculated as:

$$p^{loss} = \sum_{i\in\mathcal{N}}\left(p_i^{D,sp} + f_i^c P_i^R - P_i^L\right) \quad (2)$$

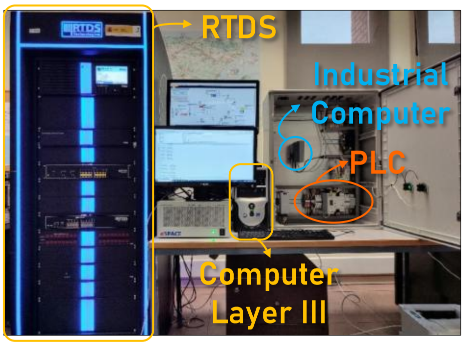

Fig. 2. Hardware architecture of the RTOLab environment

where $\Delta p_i^{D,up}$ represents upward redispatch of generator i, and $C_i^{D,up}$ is the associated cost coefficient.

B. Objective Function Variants for Voltage and Reactive Margin Control

As discussed in the Introduction, cost and active power losses minimization are commonly adopted objectives in both scheduling and RT optimization. While such objectives promote efficient operation, they may also drive bus voltages toward their upper admissible limits, potentially reducing operational margins and increasing sensitivity to disturbances, thereby motivating the alternative formulations presented below.

1) *Quadratic Voltage Deviation Penalty (Obj II).* The first alternative objective promotes voltage centering by penalizing squared deviations from the nominal voltage magnitude across the grid:

$$min\, f\left(\Delta p_i^{D,up}, p^{loss}, v_i\right) = \sum_{i\in\mathcal{D}} C_i^{D,up} \Delta p_i^{D,up} + p^{loss} + \alpha \sum_{i\in\mathcal{N}}\left(v_i - V_i^{ref}\right)^2 \quad (3)$$

This formulation softly discourages voltage saturation without explicitly modifying voltage limits.

2) *Minimax Voltage Deviation (Obj III).* The second variant directly limits the maximum absolute voltage deviation across all buses, which can be mathematically expressed as:

$$min\, f\left(\Delta p_i^{D,up}, p^{loss}, v_i\right) = \sum_{i\in\mathcal{D}} C_i^{D,up} \Delta p_i^{D,up} + p^{loss} + \beta \max_{i\in\mathcal{N}} \left|v_i - V_i^{ref}\right| \quad (4)$$

To enable the formulation of this objective function within the NLP problem, an additional variable, Δv_{max}, is introduced, subject to the following constraints:

$$\Delta v_{max} \geq \left(v_i - V_i^{ref}\right), \Delta v_{max} \geq \left(V_i^{ref} - v_i\right), \forall i \in \mathcal{N} \quad (5)$$

yielding the following objective function:

$$min\, f\left(\Delta p_i^{D,up}, p^{loss}, v_i\right) = \sum_{i\in\mathcal{D}} C_i^{D,up} \Delta p_i^{D,up} + p^{loss} + \beta\, \Delta v_{max} \quad (6)$$

This minimax formulation explicitly targets the worst-case voltage deviation across the grid, preventing extreme voltage excursions at individual buses.

3) *Voltage Deviation and Reactive Effort Penalization (Obj IV).* The third objective function extends the voltage deviation penalization introduced in Obj II by incorporating an additional term that penalizes reactive power utilization. In addition to the base objective, a quadratic term on generator reactive power outputs is included to discourage operating points with high reactive injections or absorptions, which are typically associated with reduced reactive power margins. The resulting objective function is expressed as:

$$min\, f\left(\Delta p_i^{D,up}, p^{loss}, v_i, q_i\right) = \sum_{i\in\mathcal{D}} C_i^{D,up} \Delta p_i^{D,up} + p^{loss} + \alpha \sum_{i\in\mathcal{N}}\left(v_i - V_i^{ref}\right)^2 + \gamma \sum_{i\in\mathcal{G}}\left(q_i - Q_i^{G,ref}\right)^2 \quad (7)$$

C. Constraints of the Optimization Model

Each objective function presented above is complemented by the constraints presented below:

$$p_i^{D,sp} + f_i^c P_i^R - P_i^L = v_i \sum_{k \in \mathcal{N}} Y_{ik} v_k \cos(\theta_i - \theta_k - \varphi_{ik}), \forall i \in \mathcal{N} \quad (8)$$

$$p_i^{D,sp} = P_i^{D,sch} + \Delta p_i^{D,up} - \Delta p_i^{D,down}, \forall i \in \mathcal{D} \quad (9)$$

$$q_i - Q_i^L = v_i \sum_{k \in \mathcal{N}} Y_{ik} v_k \sin(\theta_i - \theta_k - \varphi_{ik}), \forall i \in \mathcal{N} \quad (10)$$

$$V_i^{min} \leq v_i \leq V_i^{max}, \forall i \in \mathcal{N} \quad (11)$$

$$P_i^{D,min} \leq p_i^{D,sp} \leq P_i^{D,max}, \forall i \in \mathcal{D} \quad (12)$$

$$Q_i^{G,min} \leq q_i \leq Q_i^{G,max}, \forall i \in \mathcal{G} \quad (13)$$

$$i_{ik}^2 = Y_{ik}^2 (v_i \cos\theta_i - v_k \cos\theta_k)^2 + Y_{ik}^2 (v_i \sin\theta_i - v_k \sin\theta_k)^2, \ \forall (i,k) \in \mathcal{N} \quad (14)$$

$$0 \leq i_{ik} \leq I_{ik}^{max}, \forall (i,k) \in \mathcal{N} \quad (15)$$

$$-\pi \leq \theta_i \leq \pi, \forall i \in \mathcal{N} \quad (16)$$

$$\theta_{bus,ref} = 0 \quad (17)$$

Active (8)-(9) and reactive (10) power balance equations are enforced at each bus. Operational limits include bounds on bus voltage magnitudes (11), generator active (12) and reactive (13) power capabilities, and line thermal limits (14), (15). Lastly, voltage angle bounds are enforced by constraint (16), whereas constraint (17) specifies the system slack bus. Renewable generation is modeled through forecasted available power, with curtailment allowed when required by grid or operational constraints.

The decision variables include bus voltage magnitudes and angles, generator reactive power outputs, corrective redispatch actions relative to the scheduled operating point, and renewable generation curtailment. Corrective active-power redispatch is explicitly modeled through up- and down-regulation variables that quantify deviations from the scheduled setpoints (market/EMS). This formulation ensures that the optimization operates as a RT corrective layer rather than a full rescheduling mechanism.

4. Case Study and Experimental Design

A. Lanzarote–Fuerteventura Power System

The proposed RT optimization framework is assessed using a model of the Lanzarote-Fuerteventura isolated power system, which represents a realistic medium-sized islanded grid. The system consists of two main islands interconnected by two submarine cables and includes conventional generation units on each island, as well as wind and photovoltaic (PV) RES. In addition, a battery energy storage system (BESS) is included in the RTOLab experiments to investigate alternative control strategies. Dispatchable generators are equipped with voltage control functionality, while renewable generation units provide reactive power control capabilities, enabling the evaluation of alternative reactive power operating strategies.

A single-line diagram of the system is shown in Fig. 3, highlighting the considered generation nodes along with their respective nominal power ratings and the interconnection corridors. In Layer I, the system is

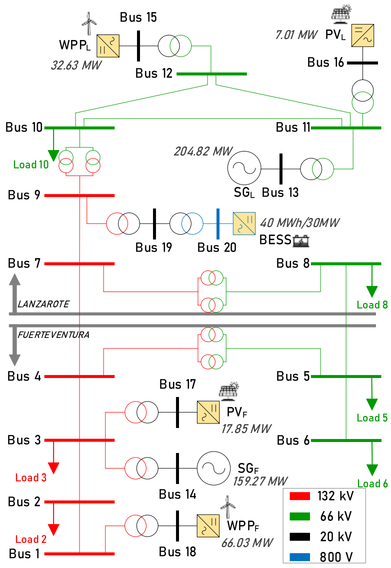

Fig. 3. Single-line diagram of the Lanzarote-Fuerteventura power system

represented through the parameters of the optimization model, whereas in Layer III it is modeled using detailed EMT models. Load and generation profiles are derived from realistic data provided by the transmission system operator (TSO).

B. Real-Time Experimental Setup

The RT experiments are conducted over a 24-hour operating period using identical load demand and renewable generation profiles, along with the same model parameters, for all evaluated cases. The RT optimization is executed every 5 minutes, resulting in 288 optimization instances per scenario. This setup enables a consistent comparison of the impact of the objective function design on the resulting RT operating point.

Four scenarios are evaluated: case i) the base case, using the loss and redispatch cost minimization objective, Obj I; case ii) including the quadratic voltage deviation term through Obj II; case iii) using Obj III, based on the minimization of the maximum absolute voltage deviation; and case iv), extending Obj II with an additional term promoting reactive power margin preservation: Obj IV.

The weighting factors α, β, γ are all set to 1, so that differences across cases are solely due to the structure of the objective function. Weight tuning is left for future work. For the purposes of this study, voltage limits are set to an admissible range of 0.95-1.05 p.u. for all buses, V_i^{ref} set to 1 p.u. and Q_i^{ref} is set to 0 pu.

5. Results and discussion

This section compares the impact of the proposed objective-function variants on the RT operation over the 24-hour period. All optimization instances are solved within the 5-minute interval, with solution times below 1 second and no infeasible cases. The analysis focuses on voltage behavior, system losses, reactive power margin, and a steady-state robustness indicator.

Fig. 4 shows the evolution of bus voltage magnitudes for all buses and all cases. In the base case, voltage profiles are pushed towards the upper admissible limit, with several buses operating at 1.05 p.u. for extended periods. This confirms that losses minimization exploits voltage-dependent loss reductions and leads to operating points near the voltage constraint boundary.

Introducing voltage-related terms in the objective function significantly modifies this behavior. The quadratic voltage deviation penalty (Obj II) results in more centered voltage profiles, reducing high-voltage regions without explicitly tightening voltage limits. However, some dispersion remains, as this formulation penalizes average deviations rather than explicitly controlling extreme values. The maximum voltage deviation minimization objective function (Obj III) provides the most effective control over the extreme voltage value. As shown in Fig. 4, the maximum voltage is significantly reduced compared to the base case and Obj II. This confirms that explicitly targeting the worst-case deviation is an effective strategy to prevent voltage saturation. The combined voltage deviation and reactive effort penalization (Obj IV) yields intermediate voltage profiles, avoiding systematic saturation while relaxing the strict voltage control enforced by Obj III.

These trends are summarized in Table I. Obj III reduces the maximum voltage over the studied period to 1.037 p.u., whereas maximum voltages reach 1.05 p.u. for Obj I and IV, although less systematically in the latter, and remain close to the upper admissible limit for Obj II. As expected, loss minimization yields the lowest system losses. This trend is consistently observed across all evaluated periods, where the base case always presents the minimum losses, followed by Obj IV. In contrast, voltage-focused objectives (Obj II and Obj III) introduce a moderate increase of approximately 2–3 MWh over the 24-hour period, indicating that controlling voltage deviations, either in an average or worst-case sense, comes at a comparable energetic cost.

Fig. 5 presents the aggregated reactive power utilization of all generators. Lower values indicate operating points closer to zero reactive power output, which are associated with increased reactive headroom. Although the differences in this study are not pronounced, the baseline case exhibits the

Table I. - System Performance Metrics for the Analyzed Cases

Case Study	Base Case	Obj II	Obj III	Obj IV
Min.Voltage (p.u.)	0.9780	0.9684	0.9629	0.9673
Max.Voltage (p.u.)	1.0500	1.0499	1.0371	1.0500
Losses (MWh)	53.0692	55.9964	55.9453	54.3502
Red. Cost (m.u.)	118.7115	119.8432	119.9666	119.1377

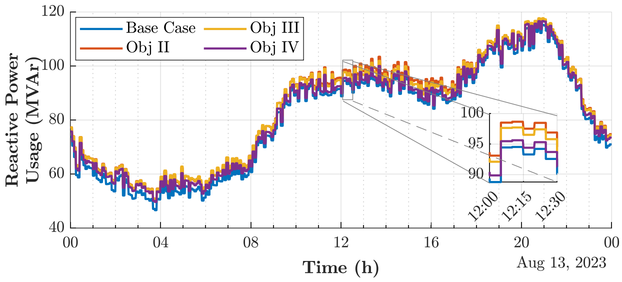

Fig. 5. Total reactive power utilization over the 24-hour period

lowest aggregated reactive power utilization throughout the day. However, this result is achieved by operating close to the upper voltage limit. Obj IV consistently reduces reactive power utilization compared to Obj II and Obj III, exhibiting the second-lowest utilization across all hours of the day. This confirms the effectiveness of the reactive effort penalization term included in its objective function. This formulation discourages large reactive injections or absorptions and promotes a more balanced use of reactive resources at the system level. Comparing Obj. II and Obj. III, Obj. III exhibits lower reactive power utilization in 66.67% of the evaluated periods.

Finally, Fig. 6 shows the minimum eigenvalue of the power-flow Jacobian evaluated at each optimal operating point. The magnitude of the eigenvalue associated with a given mode indicates the degree of stability of that mode: negative eigenvalues indicate voltage instability, while smaller positive eigenvalues denote modes that are closer to instability. Offline studies of the system indicate that when the minimum eigenvalue falls below approximately 0.55, it decreases significantly faster with increasing system load than for higher eigenvalue levels. Accordingly, in all cases, the system remains stable and operates far from the voltage collapse proximity point. The base case presents the highest eigenvalues, indicating a larger margin against voltage collapse; however, this is

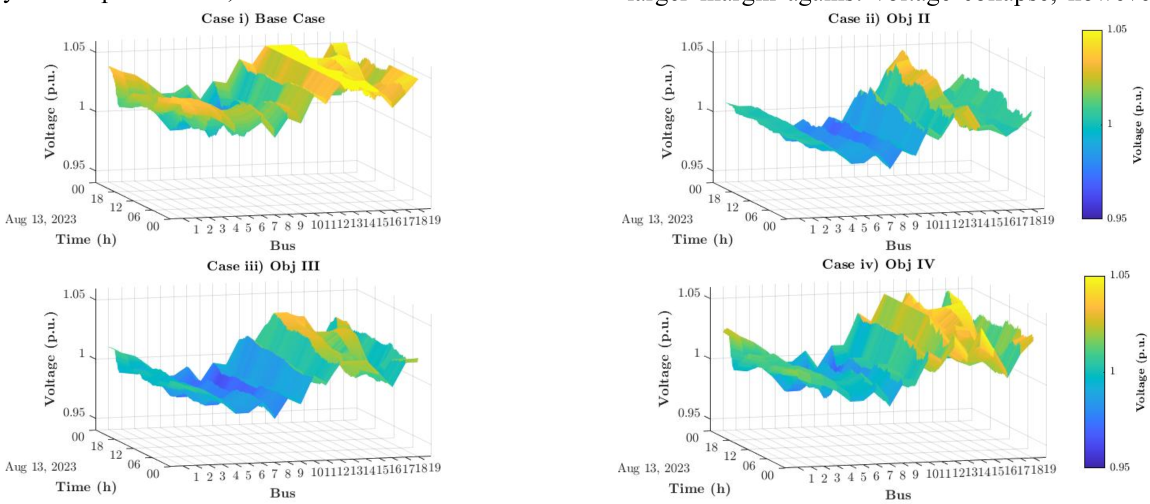

Fig. 4. Bus voltage profiles over the 24-hour operating period

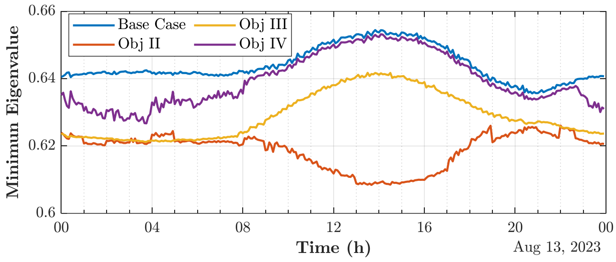

Fig. 6. Minimum eigenvalue of the power-flow Jacobian over the 24-hour operating period

associated with operation at voltage levels close to the upper limits, which may increase the risk of overvoltage tripping. In contrast, Obj II exhibits the lowest values, particularly during high-load periods. Obj III improves this indicator by limiting extreme voltage deviations. Obj IV achieves eigenvalue trajectories close to those of the base case, while avoiding persistent voltage saturation.

6. Conclusion

This paper investigates the impact of the objective function on an optimization-based RT control strategy acting as a corrective layer below an external active-power setpoint scheduling process. Results obtained in a RT optimization framework implemented in RTOLab show that losses and redispatch cost minimization systematically drives the voltages of certain buses toward their upper admissible limits, resulting in voltage-saturated operating points.

Several alternative objective functions have been analyzed to mitigate this behavior without introducing additional constraints. Penalizing voltage deviations from the nominal value reduces voltage saturation, while minimizing the maximum voltage deviation provides the most effective control over the extreme voltage value. However, these voltage-focused formulations introduce moderate increases in system losses and, in some operating conditions, higher reactive power utilization. By combining voltage deviation penalization with a reactive effort term, Obj IV provides a balanced compromise. Although operation at the upper voltage limit is not completely avoided, persistent voltage saturation is mitigated, reactive power utilization is reduced compared to purely voltage-driven objectives, and a steady-state robustness indicator based on the minimum eigenvalue of the power-flow Jacobian is improved, with a limited impact on system losses.

These results highlight the relevance of objective-function design in RT-OPF applications and show that small modifications to the objective structure can significantly affect voltage behavior, reactive power usage, and robustness metrics. Future work will address closed-loop RT analysis and adaptive weighting strategies.

Acknowledgement

This work has been supported by the EU-funded i-STENTORE Project (Grant agreement ID: 101096787) and by the Spanish Research Agency under Grant PID2022-140327OB-I00: “Mejora de la estabilidad de los sistemas eléctricos mediante generadores síncronos virtuales basados en convertidores grid-forming. Aplicación al sistema eléctrico Balear”. The authors wish to thank “Comunidad de Madrid” for the financial support provided to the PREDFLEX-CM project (TEC-2024/ECO-287), through the R&D activities programme “Tecnologías 2024”.

References

[1] J. Wang, J. Comden, and A. Bernstein, *Real Time–Optimal Power Flow–Based Distributed Energy Resource Management System (DERMS)*, Golden, CO, USA: National Renewable Energy Laboratory (NREL), Tech. Rep. NREL/TP-5D00-87767, May 2024.

[2] E. Mohagheghi, M. Alramlawi, A. Gabash, and P. Li, “A survey of real-time optimal power flow,” *Energies*, vol. 11, no. 11, Art. no. 3142, 2018, doi: 10.3390/en11113142.

[3] Z. Yan and Y. Xu, "Real-Time Optimal Power Flow: A Lagrangian Based Deep Reinforcement Learning Approach," in *IEEE Transactions on Power Systems*, vol. 35, no. 4, pp. 3270-3273, July 2020, doi: 10.1109/TPWRS.2020.2987292.

[4] P. A. Dratsas, G. N. Psarros, and S. A. Papathanassiou, “A real-time redispatch method to evaluate the contribution of storage to capacity adequacy,” *IEEE Transactions on Power Systems*, vol. 39, no. 1, pp. 1274–1284, Jan. 2024, doi: 10.1109/TPWRS.2023.3243669.

[5] C. M. Martín, F. Arredondo, S. Arnaltes, J. Alonso-Martínez and J. L. R. Amenedo, "Optimal Re-Dispatch and Reactive Power Management in the Fuerteventura-Lanzarote Grid Using Real-Time Optimization in the Loop," in *2024 IEEE 15th International Symposium on Power Electronics for Distributed Generation Systems (PEDG)*, Luxembourg, Luxembourg, 2024, pp. 1-6, doi: 10.1109/PEDG61800.2024.10667466.

[6] O. S. T. A. Butti, M. Burunkaya, J. Rahebi and J. M. Lopez-Guede, "Optimal Power Flow Using PSO Algorithms Based on Artificial Neural Networks," in *IEEE Access*, vol. 12, pp. 154778-154795, 2024, doi: 10.1109/ACCESS.2024.3479097.

[7] Y. Tang, K. Dvijotham and S. Low, "Real-Time Optimal Power Flow," in *IEEE Transactions on Smart Grid*, vol. 8, no. 6, pp. 2963-2973, Nov. 2017, doi: 10.1109/TSG.2017.2704922.

[8] L. Rouco, F. M. Echavarren, and E. Lobato, “The overvoltage-driven blackout of the Iberian Peninsula on 28th April 2025,” *Sustainable Energy, Grids and Networks*, vol. 45, Art. no. 102125, 2026, doi: 10.1016/j.segan.2026.102125.

[9] E. Mohagheghi, A. Gabash, M. Alramlawi, and P. Li, “Real-time optimal power flow with reactive power dispatch of wind stations using a reconciliation algorithm,” *Renewable Energy*, vol. 126, pp. 509–523, 2018, doi: 10.1016/j.renene.2018.03.072.

[10] K. Khatua and N. Yadav, “Voltage stability enhancement using VSC-OPF including wind farms based on genetic algorithm,” *International Journal of Electrical Power & Energy Systems*, vol. 73, pp. 560–567, 2015, doi: 10.1016/j.ijepes.2015.05.007.

[11] M. Ntombela, K. Musasa, and M. C. Leoaneka, “Power loss minimization and voltage profile improvement by system reconfiguration, DG sizing, and placement,” *Computation*, vol. 10, no. 10, Art. no. 180, 2022, doi: 10.3390/computation10100180.

[12] P. Mundra, A. Arya, and S. K. Gawre, “A multi-objective optimization based optimal reactive power reward for voltage stability improvement in uncertain power system,” *Journal of Electrical Engineering & Technology*, vol. 16, pp. 1–13, 2021, doi: 10.1007/s42835-021-00827-0.

[13] S. S. Reddy and P. R. Bijwe, “Day-ahead and real time optimal power flow considering renewable energy resources,” *International Journal of Electrical Power & Energy Systems*, vol. 82, pp. 400–408, 2016, doi: 10.1016/j.ijepes.2016.03.033.